Current Research in Food Science 8 (2024) 100670

Contents lists available at ScienceDirect

Current Research in Food Science

journal homepage: www.sciencedirect.com/journal/current-research-in-food-science

The influence of cooperative fermentation on the structure, crystallinity, and rheological properties of buckwheat starch

Xia Li [1], Shanshan Wei [1], Zixin Gao, Ruixue Zhao, Zhanpeng Wang, Yuling Fan, Linlin Cui, Yuhua Wang [*]

College of Food Science and Engineering and Jilin Province Innovation Center for Food Biological Manufacture, Jilin Agricultural University, Changchun, Jilin Province, 130033, China

ARTICLE INFO

Handling editor: Xing Chen

Keywords:
Lactic acid bacteria
Amylose content
Physical properties
Buckwheat starch

ABSTRACT

The effects of co-fermentation of yeast and *Lactiplantibacillus plantarum* 104 on buckwheat starch physical properties were investigated by various analytical techniques. To investigate the regulations of starch modification during fermentation and to provide a foundation for improving the performance of modified properties of buckwheat starch food. The pasting properties were decreased by co-fermentation also resulted in a reduction in the relative crystallinity. Scanning electron microscopy (SEM) demonstrated that more holes and a relatively rough granule surface were seen in the co-fermentation group. Fourier transform-infrared spectroscopy (FT-IR) results suggested that co-fermentation fermentation decreased the degree of short-range order (DO) and degree of t[1]he double helix (DD). The results demonstrated that co-fermentation altered these properties more rapidly than spontaneous fermentation. In conclusion, *Lactiplantibacillus plantarum* 104 could be used for buckwheat fermentation to improve food quality.

1. Introduction

Fermented flours-based foods attract more consumers due to their ability to improve properties such as digestibility, emulsification, stability, swelling, cooking characteristics, and gel properties compared with those made from non-fermented flours. However, the time taken to spontaneously ferment dough is too long, limiting the development and application of this method. Lactic acid bacteria play a crucial role in fermentation as they produce various substances that can impact the cereal raw materials being fermented. Additionally, some lactic acid bacteria strains have been shown to have the ability to improve the oxidation resistance of plant-based foods. This can be particularly beneficial as oxidation has positive effects on the color, flavor, and nutritional profile of food products. Therefore, lactic acid bacteria fermentation offered insights into improving the properties of naturally fermented doughs.

Yeast can play an important role in the fermentation of dough. During fermentation, yeast produces pyruvic acid, vitamins, and amino acids, which can be utilized by lactic acid bacteria for their metabolic activities. Lactic acid bacteria produce organic acids, ethanol, and other important enzymes that contribute to the flavor, texture, and overall quality of pasta (Sun et al., 2022). The synergistic interaction between yeast and lactic acid bacteria during fermentation results in improved dough elasticity and viscosity, as well as increased nutritional value and sensory properties of the final product (Heitmann et al., 2015).

Buckwheat is classified as a pseudocereal and has been cultivated and consumed worldwide due to its great ecological adaptability and ability to grow in almost all kinds of extreme environments. Buckwheat is rich in vitamins, including thiamin, riboflavin, pyridoxine, and minerals (Sun et al., 2022). As a result, it was well recognized as a potential functional food source in some countries. However, local buckwheat flour is poor in clumping, which limited its development and has inferior processing characteristics, buckwheat starch is less transparent, and the aging rate is faster compared to maize and potato. Therefore, it was important to explore ways to improve the processing properties of buckwheat flour.

The starch content in buckwheat flour was 60–70% and plays a key role in the development of pasta with beneficial processing properties (Cheng et al., 2020). The structural properties of starch affect its thickening ability, stability, and gelatinization. Many studies have

* Corresponding author.
E-mail address: yuhua-ww@163.com (Y. Wang).
[1] These authors contributed equally to this article.

https://doi.org/10.1016/j.crfs.2023.100670
Received 4 October 2023; Received in revised form 18 December 2023; Accepted 25 December 2023
Available online 30 December 2023

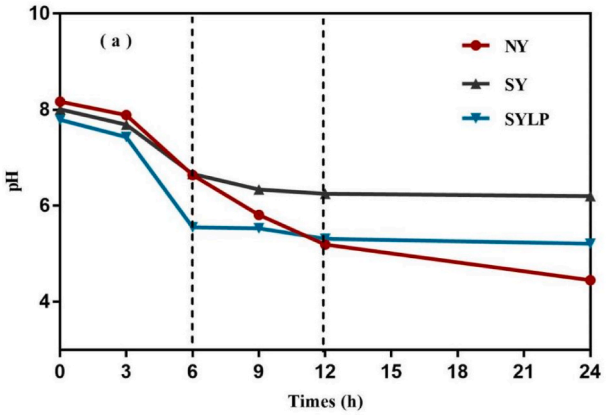

Fig. 1. pH of the buckwheat starch slurry. Spontaneous fermented (NY), yeast fermented (SY), yeast and *Lactobacillus plantarum* 104 co-fermented (SYLP) buckwheat starch at different fermentation times.

shown that the internal molecular structure influences the starch physicochemical properties. The literature stated that starch amylose content determines their heating and pasting properties (Zabot et al., 2019). The relative crystallinity was related to the starch paste viscosity (Zhou et al., 2021). These studies aimed to clarify the correlation between internal molecular structure, physical, and chemical properties. However, the effect of co-fermentation and its duration on structural changes in buckwheat starch remains unclear.

This study aims to investigate the effects of yeast and *L. plantarum* co-fermentation at different times on buckwheat starch structural and physical properties, including amylose content, short-range ordered structure, morphological characteristics, crystal structure, pasting properties, rheological and thermomechanical characteristics of buckwheat starch. The results of this study can be used to improve properties of modified buckwheat related food products.

2. Materials and methods

2.1. Materials

The buckwheat was procured from Baicheng Taobei District Commercial Street, Jilin Province (China). The dehulled common buckwheat grains removed shriveled and damaged grains was milled into flour by lab flour machine (Herb Grinder, Yongkang Hardware Products Co., Lt, Zhejiang, China). *L. plantarum* 104 (LP104) was selected from the China Type Culture Collection (CCTCC No. M20190843; Wuhan, China). The strain was activated and cultivated at 37 °C, then inoculated for fermentation. Yeast (highly active dry yeast) was purchased from Jilin Qishen Foods Company, Ltd (Jilin, China).

2.2. Sample preparation

LP104 (2% v/v) was inoculated into MRS broth and cultured (37 °C, 24 h), and then centrifuged (3500 g, 15 min) to isolated bacterial sludge. The concentration of LP104 cells gained was adjusted to 10^8 CFU/mL with sterile water. Starch was isolated using the method described by Xin Bian and Lei Sun and made improvements accordingly (Bian et al., 2022; Sun et al., 2022). Spontaneously fermented dough (labeled "NY") was prepared as follows: buckwheat flour (80 mesh) and distilled water were added in a ratio of 5:3 (w/v) and spontaneously spontaneous fermented for 0 h, 6 h, 12 h and 24 h respectively. The starch fermented by yeast (labeled "SY"), mixed using the same proportions, and added 0.4 g of yeast fermented for 6 h, 12 h and 24 h respectively. The co-fermented starch (labeled "SYLP") contained the same proportion of buckwheat flour and LP104 suspension with an additional 0.4 g of yeast fermented at 37 °C for 6, 12, and 24 h. The fermented buckwheat dough was mixed with distilled water. After stirring at room temperature for 5 min, the mixture was run through a 150-mesh nylon cloth to separate fiber and other impurities to produce starch slurry, and then centrifuged at 5000 rpm for 10 min, removed supernatant. The starch pellet was washed several times with distilled water until it was free of impurities and then dried at 40 °C for 12 h. The dried starch passed through a 100-mesh sieve to obtain a uniform particle size. The starch was stored in drying containers at room temperature.

2.3. Determination of pH

The pH of the natural starch slurry and the different fermentation treatments of starch slurry were measured using a pH meter (SE-S400-K) at different fermentation times (0 h, 6 h, 12 h and 24 h).

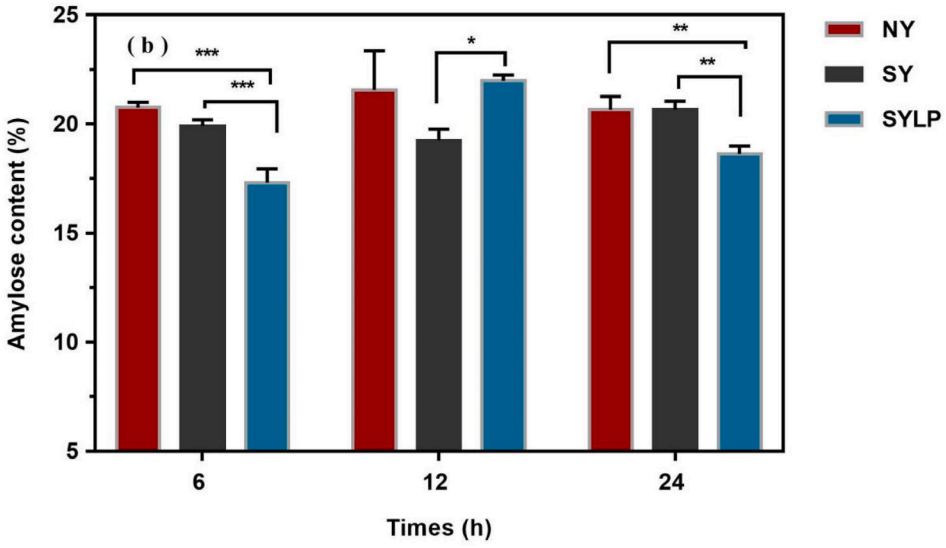

Fig. 2. Effect of fermentation on amylose content of buckwheat starch. Spontaneous fermented (NY), yeast fermented (SY), yeast and *Lactobacillus plantarum 104* co-fermented (SYLP) buckwheat starch at different fermentation times. *p < 0.05, **p < 0.01, ***p < 0.001 indicate the significant differences between different groups.

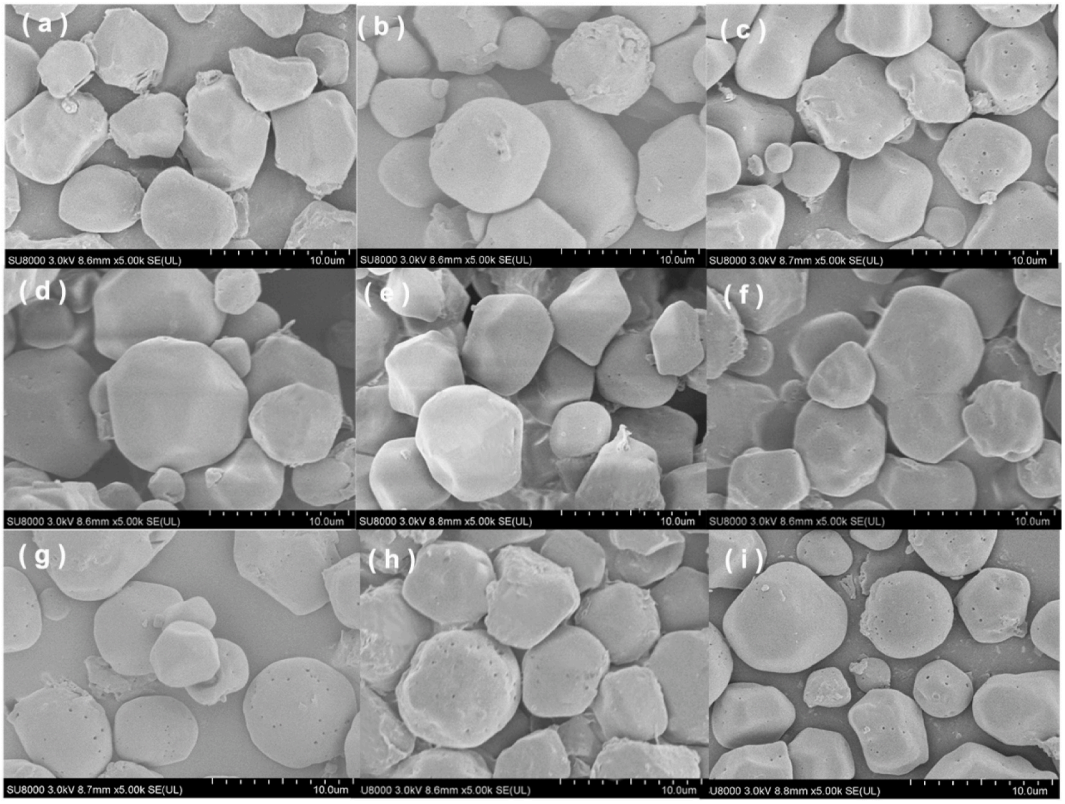

Fig. 3. Scanning electron micrographs of NY, SY, and SYLP buckwheat starch at different fermentation times. (a) NY 0 h, (b) NY 12 h, (c) NY 24 h, (d)SY 6 h, (e) SY12 h, (f) SY:24 h, (g) SYLP: 6 h, (h) SYLP 12 h, and (i) SYLP 24 h at a magnification of 5000 × .

2.4. Apparent amylose content

The apparent amylose content was determined according to previous a study with some modifications (Dar et al., 2018). The sample amylose content was determined by iodine colorimetry (GBT15683).

2.5. Scanning electron microscopy (SEM)

The starch sample was placed on the tape of an aluminum specimen column and then the starch sample was coated with gold particles for 90s with the MSP-1S sputter coater. Observation of buckwheat starch morphological properties using scanning electron microscopy. Microstructures of different buckwheat starch samples were captured at the magnification of × 5000 by SEM (TM3000, Hitachi Ltd., Tokyo, Japan).

2.6. Fourier transform infrared (FTIR) analysis of buckwheat starch

FTIR was performed using the method described by Xin Bian et al. (2022). The dried buckwheat starch samples were mixed with a KBr pellet, then, the samples were pressed into tablets, and examined using an infrared spectrometer. The scan range is 4000–500 cm-1, and the origin software was used to adjust the baseline and determine the position of the absorption peaks.

2.7. X-ray diffraction analysis of buckwheat starch

The crystal structures of the samples from the different fermentation treatments were determined by the Terra-2 polycrystalline diffractometer (Quanze, China), running at 40 kV and 30 mA in the range of 5–40° (2θ, 5°/min). The effect of the fermentation treatment on the crystallinity of the starch was observed. The relative crystallinity was determined using Origin 2021 software according to the following equation:

$$RC = \frac{Ac}{Ac + Aa} \times 100\% \quad (1)$$

where the RC value represents the relative crystallinity of the buckwheat starch, Ac and Aa represent the area under the amorphous and crystalline regions of the spectrum, respectively.

2.8. Pasting properties of buckwheat starch

The rapid viscosity analyzer (RVA) was used to assess the pasting qualities of buckwheat starch (Kong et al., 2020). The sample is placed in a rapid viscosity analysis for determination. Gelatinization temperature (GT), the viscosity value of peak (PV), trough (TV), breakdown (BD), final (FV), and setback (SB) were determined.

2.9. Thermal properties of buckwheat starch

The thermal properties of the unfermented and fermented buckwheat starch were observed by DSC7020 instrument (Hitachi High-Tech., Touhotu, Japan). The starch of samples (3 mg) was weighed and placed in an aluminum pan, and distilled water was added to achieve a moisture level of 70%, the samples were mixed evenly, and sealed. After sealing, the crucible was balanced at room temperature for 24 h. With an empty crucible as a reference, nitrogen (flow rate is 50 ml/min) was introduced, and the temperature was gradually increased from 30 °C to 120 °C at a rate of 10°/min. Data were recorded for the onset temperature (To), peak temperature (Tp), conclusion temperature of the gelatinization (Tc), and gelatinization enthalpy (ΔH).

2.10. Rheological properties of the starch paste

The dynamic Rheology of the starch paste used in the above experiments was determined using a Modular Compact Rheometer (Anton

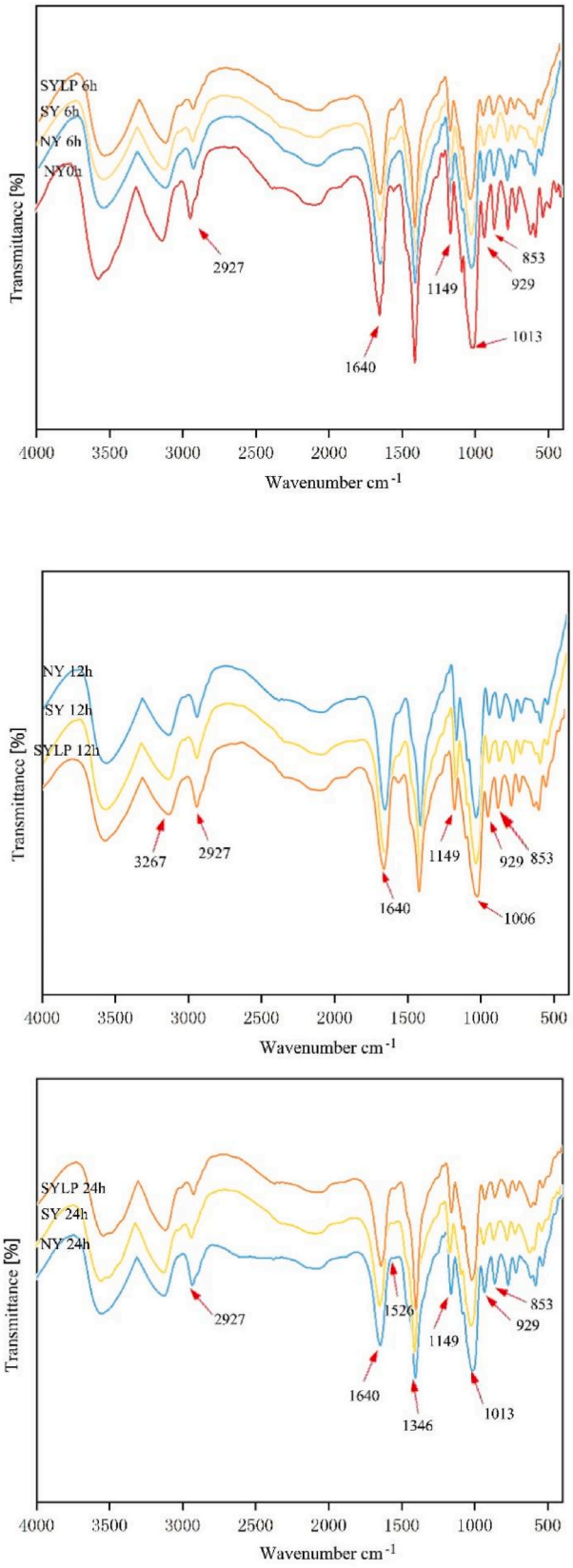

Fig. 4. FTIR spectra of different fermented treatment buckwheat starch at different fermentation times.

Paar, Austria), and modified the previous method equipped with parallel plate system (Singh and Kaur, 2017). Cool the starch paste prepared according to the above section approximately room temperature (25 °C) for further rheological testing. The dynamic rheological parameters of starch were determined, including storage modulus (G′), loss modulus (G″) and loss factor (tanδ). The dimensionless parameter tanδ determined from G''/G', which provides a precise indication of the viscoelasticity of samples. The shear stress (τ) and shear rate (γ) of the starch paste were recorded in a continuous shear experiment. The resulting flow profiles were described using the Ostwald–de Waele rheological model.

$$\tau = k \bullet \dot{\gamma}^{n} \quad (2)$$

where τ stands for the shear stress [Pa • s], *K* remains the consistency coefficient [Pa • s^n], $\dot{\gamma}$ denotes the shear rate [s^{-1}], and *n* represents the flow behavior index [−].

2.11. Statistical analysis

All statistical analyses were performed based on three parallel sets of experiments. All figures were drawn using Origin 9.0 software. Data were examined for significance using ANOVA in SPSS PASW Statistics v19.0, means and standard errors obtained and displayed as coordinates. pairs and error bars in the graphs. The difference was significant when the aggregate p-value for an experiment was less than the significance level ($p < 0.05$).

3. Results and discussion

3.1. Effect of cooperative fermentation on pH of buckwheat flour slurry

As shown in Fig. 1a, the pH values showed a downward trend under all three fermentation methods. The fermentation decreased rapidly before 6 h of SY and SYLP, and slowly after 6 h, pH decreased rapidly before 12 h of NY and slowly after 12 h, while, the pH in the first 6 h of the SYLP group was significantly lower than NY 6 h and SY 6 h groups. A previous study has proved that the cooperative fermentation of yeast and lactic acid bacteria can increase the number of live bacteria, at the same time, the yeast can promote the lactic acid bacteria to produce more lactic acid, propionic acid, acetic acid, and caseate (Han and Du, 2023). In this experiment, the SYLP group may generate more organic acids, which significantly lowers pH. The pH of the SYLP group was significantly higher than the NY group from 12 to 24 h, nevertheless. According to one proposal (Ferreira et al., 2022) The competitive growth of bacteria and yeast reduced the amounts of fermentable sugars and prevented the synthesis of organic acids, which prevents the pH of the SYLP group from dropping. As the temperature decreases following gelatinization, the hydrogen link between the adjacent molecules returns to create a dense, highly crystalline starch molecule microcrystal beam, which is referred to as starch aging (Yashini et al., 2022); pH is one of the elements that influenced starch aging. Studies showed that starch cannot recrystallize under either acidic or alkaline environments. different pH levels, however, also have an impact on the characteristics of starch paste, consequently different additives are employed to regulate pH in food processing.

3.2. Effect of cooperative fermentation on amylose content of buckwheat starch

The apparent amylose content (AAC) of the buckwheat transformed significantly with the fermentation conditions change. For natural buckwheat starch, AAC was found to be 17.32–21.98% at the time of 6 h, 12 h, and 24 h fermentation treatment (Fig. 2). Compared with the natural fermentation and yeast groups, the amylose content significantly decreased in the SYLP group in 6 h ($p < 0.001$). Moreover, starch aging

Table 1
Short-range order (DO), and Degree of the double helix (DD), Pasting properties, Thermal properties, and Gel textural parameters of NY, SY, and SYLP fermented starches.

	sample	NY 0 h	NY 6 h	NY 12 h	NY 24 h	SY 6 h	SY 12 h	SY 24 h	SYLP6h	SYLP 12 h	SYLP 24 h
FT-IR	1047/1022	1.37 ± 1.2^{a}	1.59 ± 0.04^{b}	1.50 ± 0.07^{b}	1.45 ± 0.04^{a}	1.35 ± 0.0^{a}	1.59 ± 0.03^{b}	1.33 ± 0.1^{a}	1.28 ± 0.0^{bc}	1.35 ± 0.1^{a}	1.28 ± 0.1^{acd}
	955/1022	4.17 ± 1.3^{a}	9.20 ± 1.1^{b}	6.73 ± 2.0^{d}	8.10 ± 1.5^{bd}	4.47 ± 0.1^{c}	7.78 ± 0.2^{a}	5.36 ± 2.4^{abcd}	4.51 ± 1.5^{abcd}	5.25 ± 0.1^{abcd}	3.93 ± 1.5^{ac}
RVA	PV(cP)	3643 ± 153.0^{e}	3406 ± 51.9^{de}	3038 ± 26^{c}	3176 ± 277.1^{bcd}	3085 ± 237.8^{bcd}	3653 ± 255.6^{e}	3105 ± 183.5^{bcd}	2564 ± 210.5^{a}	2826 ± 102.0^{ab}	3003 ± 116.0^{b}
	TV (cP)	3342 ± 152.9^{d}	3068 ± 70.4^{cd}	2799 ± 23.9^{bc}	2972 ± 289.5^{bc}	2851 ± 252.8^{bc}	2909 ± 292.3^{b}	2991 ± 162.0^{bc}	2402 ± 204.3^{a}	2650 ± 79.3^{ab}	2816 ± 122.0^{bc}
	BD (cP)	302 ± 6.6^{ab}	338 ± 24.3^{b}	242 ± 9.9^{ab}	204 ± 19.6^{ab}	234 ± 19.8^{ab}	944 ± 309.3^{cb}	115 ± 21.5^{a}	163 ± 6.9^{ab}	177 ± 24.9^{ab}	187 ± 6.0^{ab}
	FV(cP)	4914 ± 232.6^{c}	4312 ± 42.7^{b}	4047 ± 230.8^{ab}	4380 ± 232.4^{b}	4116 ± 419.6^{ab}	6244 ± 610.6^{e}	4210 ± 303.5^{b}	3620 ± 231.0^{a}	4087 ± 100.8^{ab}	4245 ± 117.5^{b}
	SB(cP)	1572 ± 79.6^{d}	1360 ± 36.4^{c}	1158 ± 113.2^{ab}	1408 ± 60.2^{c}	1171 ± 34.1^{ab}	3769 ± 52.3^{e}	1219 ± 141.5^{b}	1055 ± 117.2^{a}	1437 ± 39.2^{cd}	1429 ± 4.5^{c}
	GT (min)	7.0 ± 0.1^{c}	6.3 ± 0.1^{ab}	7.1 ± 0.7^{c}	6.7 ± 0.1^{bc}	7.1 ± 0.3^{c}	6.0 ± 0.8^{a}	6.8 ± 0.1^{bc}	6.9 ± 0.3^{bc}	6.8 ± 0.1^{bc}	6.7 ± 0.1^{bc}
	PT (°C)	91 ± 5.1^{bc}	87 ± 0.8^{b}	93 ± 6.5^{c}	86 ± 1.4^{b}	88 ± 0.9^{bc}	85 ± 2.8^{ab}	88 ± 0.8^{bc}	79 ± 6.6^{a}	86 ± 0.5^{bc}	87 ± 0.4^{bc}
DSC	To (°C)	59.2 ± 2.7^{a}	58.3 ± 0.9^{a}	58.2 ± 1.2^{a}	58.4 ± 0.6^{a}	59.5 ± 0.8^{a}	59.9 ± 0.4^{a}	58.4 ± 4.3^{a}	60.8 ± 2.1^{a}	61.8 ± 0.9^{a}	62.8 ± 1.8^{a}
	T_p (°C)	65.52 ± 3.0^{a}	65.3567 ± 1.0^{a}	66.28 ± 1.4^{a}	66.51 ± 0.1^{a}	66.06 ± 0.9^{a}	67.15 ± 0.4^{a}	64.95 ± 4.8^{a}	66.6567 ± 2.4^{a}	65.86 ± 1.0^{a}	66.0381 ± 1.9^{a}
	△T (°C)	−8.3 ± 0.4e^{f}	−7.8 ± 0.1^{cd}	−9.1 ± 0.2^{dg}	−8.6 ± 0.2^{f}	−7.9 ± 0.1^{e}	−9.8 ± 0.1^{h}	−7.3 ± 0.5^{b}	−7.4 ± 0.3^{bc}	−6.4 ± 0.1^{a}	−8.3 ± 0.4^{ef}
	Tc (°C)	73.2 ± 3.4^{ab}	73.2 ± 1.1^{ab}	74.5 ± 1.6^{ab}	74.4 ± 0.6^{ab}	74.0 ± 1.0^{ab}	77.3 ± 0.5^{b}	72.3 ± 5.4^{ab}	74.3 ± 2.6^{a}	71.1 ± 1.1^{a}	73.2 ± 3.4^{ab}
	△H (J/g)	−8.5 ± 0.4^{cd}	−8.1 ± 0.1^{d}	−8.8 ± 0.2^{c}	−9.3 ± 0.3^{b}	−8.4 ± 0.1^{cd}	−10.8 ± 0.1^{a}	−8.2 ± 0.6^{d}	−6.4 ± 0.2^{e}	−5.5 ± 0.1^{f}	−8.5 ± 0.4^{cd}

A: NY, SY and SYLP represents spontaneous fermented, yeast fermented, yeast and *Lactobacillus plantarum 104* fermented buckwheat starch, respectively. B: PT, PV, TV, FV, BD, SB and GT represent peak temperature, peak viscosity, trough viscosity, final viscosity, breakdown (PV-TV), setback (FV-PV) and gelatinization time, respectively. C: To, Tp, Tc, ΔT and ΔH are onset temperature, peak temperature, conclusion temperature, gelatinization temperature range (Tc-To) and enthalpy change of gelatinization, respectively. Data (mean ± SD) in the same column with different letters are significantly different ($p < 0.05$).

was divided into short-term and long-term aging, and short-term aging is affected by the rearrangement of amylose. The lower the content of amylose, the lower the degree of starch aging (Biduski et al., 2018). Some results show a decrease in amylose content after 72 h of spontaneous fermentation and 48 h of *Lactiplantibacillus plantarum* fermentation. The amorphous area of the starch granules may be affected by enzymatic (α-amylase) and acid hydrolysis processes., which led to the degradation of amylose (Bian et al., 2022) and the co-fermentation in the present experiment led to the acceleration of this reaction. The results indicated that specific changes in fermentation time increased the concentration of straight chain starch. This was consistent with the findings of Bian et al. The amylose content increased may be due to the constant generation of certain enzymes (β-amylase) or organic acids as the microorganisms keep on fermenting, resulting in the damage of some of the small chains forming amylopectin, which increased the generation of small molecules of amylose starch, resulting in an increase in amylose content. In comparison with spontaneous and yeast fermentation, co-fermentation accelerated the reaction process.

3.3. Morphology of buckwheat starch under scanning electron microscopy

The microstructure of the native and fermented buckwheat starches was given in Fig. 3. Morphological observations on the NY group show that the starch granules were relatively smooth and complete at 6 h, 12 h, 24 h, a few holes appeared on the surface (Fig. 3 d-f). Compared with SY 6 h, the starch granules at SY 12 h were coarser with a few micropores and tiny channels. Many holes and a relatively rough granule surface can also be observed in the SYLP group at 6–24 h (Fig. 3 g-i). As the pH changes shown in Fig. 1, the accumulation of organic acids increases the acidification reaction resulting in a more irregular surface of the SYLP starch granules. Microbial fermentation first destroys the surface of starch granules to form pores, and then further degrades the exterior, creating an irregular surface. Studies have shown that more pores or channels of starch granules are more prone to hydrolysis by the enzymes inherent in starch, which can affect the termination time of yeast gas production and total gas production, increasing the yeast utilization of substrate (N. Wang et al., 2020). The previous rheological results indicated that the viscosity of buckwheat starch increased after co-fermentation treatment, which may lead to the increased substrate utilization rate of yeast. Stefanie Hackenberg et al. (2018) showed that increased substrate availability positive effects prevailed over the negative effect of reduced limited diffusion due to increased stickiness.

3.4. Effect of different fermentation treatments on the short-range orderliness and crystallinity of buckwheat starch

3.4.1. FT-IR analysis of buckwheat starch

Fig. 4 presented the FTIR spectra in the range 400–4000 cm^{-1} of buckwheat starch before and after fermentation. The results showed that buckwheat starch molecular absorption peaks were similar in position and form before and after fermentation and that no new absorption peak appeared in the figure, indicating that no new compounds were formed by fermentation. The crystalline and amorphous starch structures are connected to wide bands at 1047 and 1022 cm^{-1}, respectively. The absorbance ratio at 1047/1022 cm^{-1} (R1047/1022) and 995/1022 cm^{-1} (R995/1022) were used to determine the degree of short-range order (DO) and double helix (DD). As shown in Table S1, the SYLP group exhibited lower values of R1047/1022 at the same fermentation time compared to NY and SY. In addition, a lower value of R995/1022 represented the decreased degree of the double helix. Some studies have shown the disruption of short-range ordering and double helices, which may be due to the breakage of amylose branches and the disruption of structure, more amorphous regions were formed. Similar findings from earlier research on thermally treated wheat or oat starch were reported. (Ma et al., 2021). A study reported showed that the peaks at 861 cm^{-1}-764 cm^{-1}, respectively are recognized to represent stretching

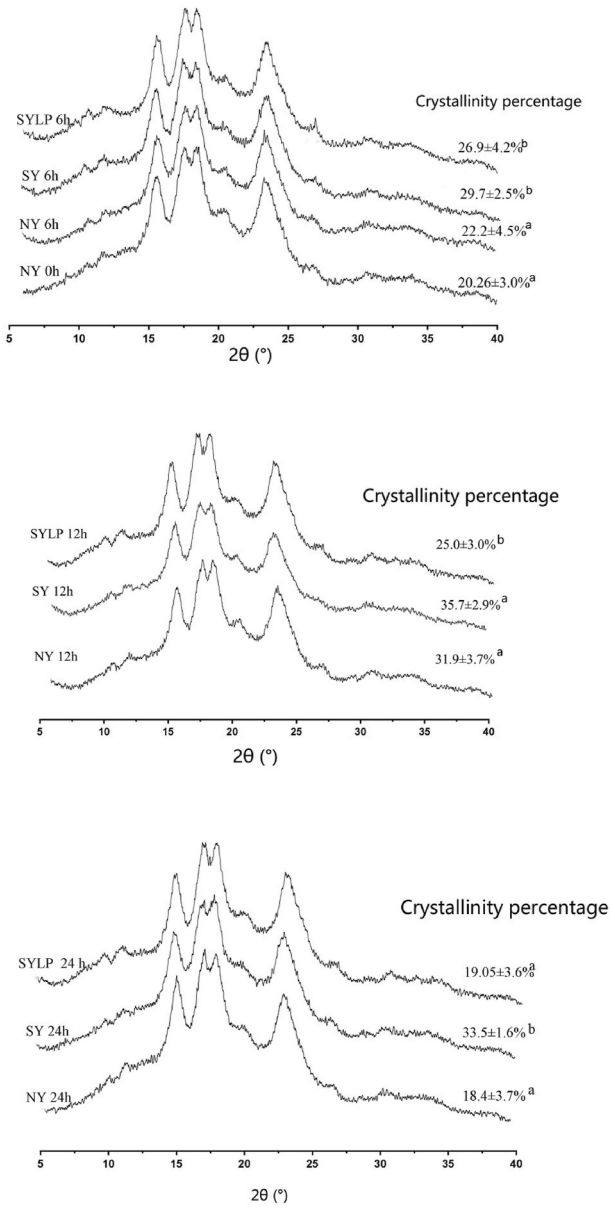

Fig. 5. XRD pattern of different fermented treatment buckwheat starch at different fermentation times.

vibration of the C–C bond and the rocking of - CH_2 - group. The glucose molecules that constitute the starch molecule all have a -CH_2 - group (methylene) (Kumar et al., 2023). When the intermolecular hydrogen bonds are weakly terminated; When the starch was in a polymerized state, the vibrational impact of the -CH_2 - group was diminished. Compared with SY 6 h group buckwheat starch, in the SYLP 6 h group, one peak of fermented starch molecule absorption was significantly increased, the impact of the free-state - CH_2 - on vibration was enhanced, as illustrated in Fig. 4, and the starch molecules were destroyed after fermentation.

3.4.2. Crystal structure of buckwheat starch

X-ray diffraction spectra (XRD) analysis (Table 1) was performed to determine the effect of different fermentation treatment on the starch structure. All of the fermented buckwheat starches displayed similar crystal properties, demonstrating that fermentation had no effect on starch crystal structure. The results also showed that the SY and SYLP groups had considerably higher starch molecule crystallinity than the NY 6 h fermentation and natural starches, as measured by the proportion of each diffraction peak to the total diffraction peak area (Fig. 5). The findings were in agreement with Sun et al. (2022) study, which may be caused hydrolysis targeted the amorphous parts more frequently. The disintegration of the amorphous area was most likely the cause of the relative crystallinity rise. However, at 12 h, the SYLP group buckwheat starch crystallinity was considerably lower than that of the other two groups. Similar results were observed in the Liu et al. (2012) investigation. The amylopectin exterior chains entangled to generate short-range ordered double helices, which were then arranged to expand into long-term ordered crystalline units, which explained the relative crystallinity increased. According to the above findings, the irregularity of the internal structural double helices may be associated to the declining trend of relative crystallinity reduction.

3.5. Effect of fermentation on the physicochemical characteristics of buckwheat starch

3.5.1. Effect on the pasting properties of buckwheat starch

The RVA analyzer was an effective instrument for determining the changes in the viscosity of starch or flour when subjected to heat and shear in water. The viscosity properties of samples were shown in detail in Table S1. The PV value was significantly reduced during the 6 h, and 12 h of SYLP fermentation, and no significant changes existed between spontaneous fermentation and yeast during 6 h, 12 h, and 24 h. Peak viscosity is related to the binding capacity of water, with higher peak viscosity and strong water binding capacity (Q. Wang et al., 2020). Setback is the recombination of inflated starch granule denotes the degree of starch short-term ageing; The retrogradation tendency was inhibited with decreasing recession and final viscosity. Compared with NY fermentations, the samples fermented by SYLP fermentation had lower setback values ($p < 0.05$) at 6 h. It indicated that the SYLP fermentation group inhibited the short-term aging of starch. In other words, cooperative fermentation can hinder short-term aging and suppress the development of starch granule gel network structure. This was consistent with the results of Ma et al. (2022). The reason may be that by 6 h of fermentation, starch molecules were very tightly linked together by the binding of water molecules and hydrogen bonding; this tendency was stronger than the ability to polymerize between starch chains, which resulted in a decrease in the setback.

The breakdown (BD) is the differential between peak and trough viscosity, expresses starch resistance to heat and shear, the smaller the value, the better the shear force and thermal stability, and the lower the degree of starch granule damage (Gui et al., 2022). Additionally, as shown in Table S1 both the SYLP fermentation groups had significantly reduced the BD value at the 6 h of fermentation ($p < 0.05$), while the decrease of SYLP group was more prominent. Marina et al. (2018) reported that enzymatic treatment of potato starch also reduced the BD value. This may be attributed to hydrolysis destroying the granular and relative crystallinity structure of the starch, which leads to a decrease in viscosity during heating (Cheng et al., 2020). In addition, the buckwheat starch network structure formed by the enzyme treatment builds a more continuous phase that hinders the recombination of straight-chain starch to supply a higher shear resistance of swollen starch granules (Wang et al., 2021). The pasting temperature can be used to determine the minimal temperature required to cook food. Compared with SY fermentation and NY fermentation, SYLP fermentation for 6 h could significantly reduce the pasting temperature of the samples ($p < 0.05$). Similar results have been reported by Zhang et al. (2019); Amylose concentration decreased along with starch breakdown, peak viscosity, final viscosity, and setback. The results also showed that the amylose content affects the pasting and gelation capabilities of starch during cooking.

3.5.2. Effect on the thermal properties of buckwheat starch

The thermal characteristics of buckwheat starch under various fermentation treatments are shown in Table S1 indicating T_0, T_P, Tc, and

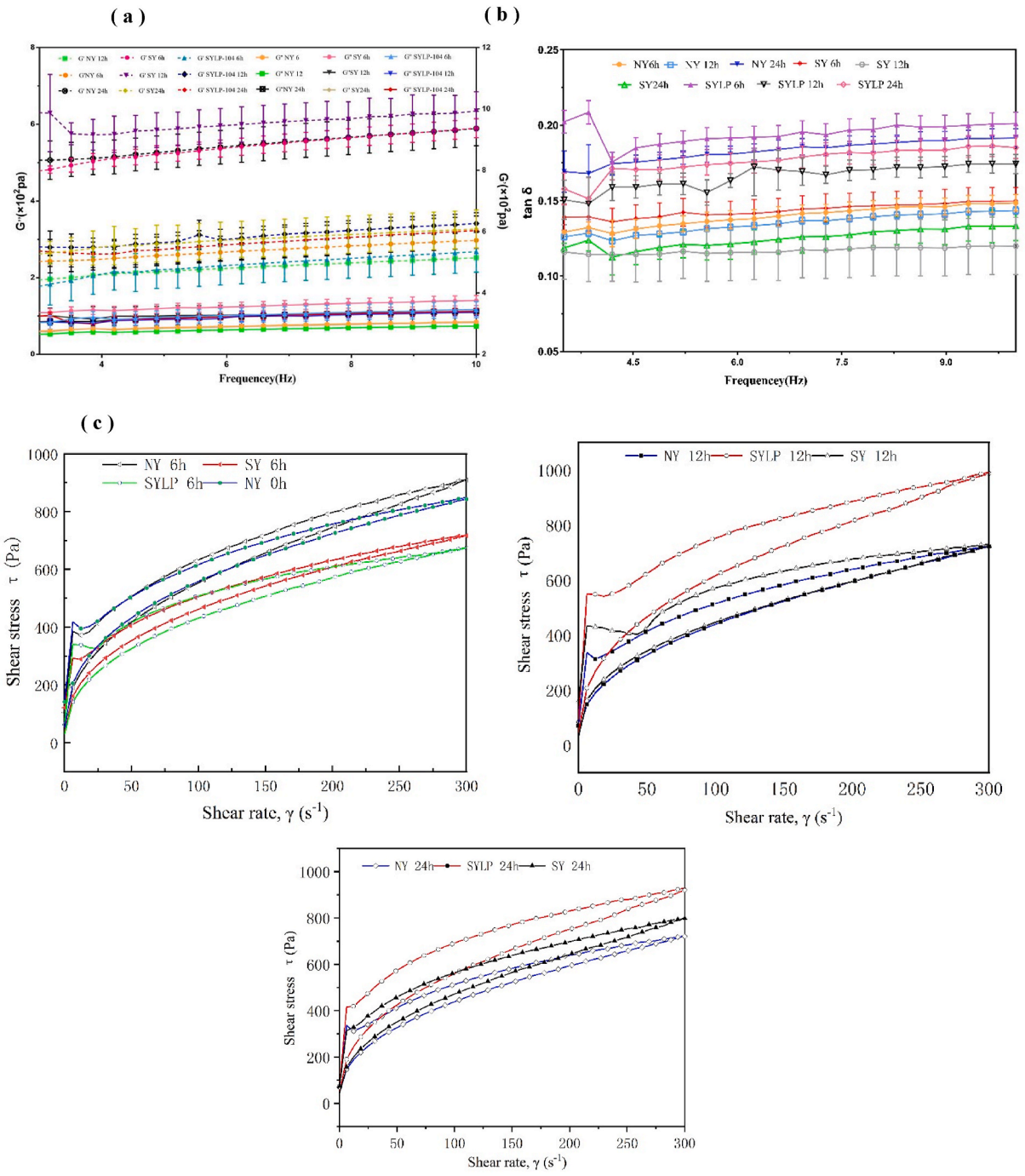

Fig. 6. Rheological characteristic of buckwheat starch. (a) Effects of different fermented treatment and fermented times on storage modulus G′, loss modulus G''. (b) tanδ (G″/G′). (c) Hysteresis curves of different fermented treatment buckwheat starch at different fermentation times.

ΔH. The To, T_p of different fermented starch with no significant differences in starch between fermentation times and methods ($p > 0.05$). In the SYLP group, ΔH also showed a trend of decreasing first and then increasing. Tc, ΔH were the lowest at 12 h in SYLP groups, which indicated that the thermal stability decreased. Tc and ΔH of buckwheat starch elevated at 24 h, The results were consistent with Kou et al. (Kou et al., 2011). This can be explained through the previous results that the amylose content first increased and then decreased at this stage (Fig. 2). ΔT is relates to the stability of the crystalline area in starch granules, and positively related to the relative crystallinity, similar to XRD results, at 12 h, the crystallinity of buckwheat starch was significantly decreased by fermentation, especially in the SYLP group ($p > 0.05$). It has been observed that ΔH was positively associated with the degradation of the double helix structure in starch crystallinity (Fonseca et al., 2021). Since the short-range molecular order mainly determined ΔH, double helix fractions, and the crystals, the decrease in ΔH indicated that fermentation treatments damaged the short-range structural order and the initial double helix structure, and the reduction of relative crystallinity, which were also consistent with R1047/1022, R955/1022 and XRD results. The results of previous studies also indicate that the crystallinity of starch decreased and the ΔH of starch pasting decreased (Molavi et al., 2018).

3.6. Effect on the rheological characteristic of buckwheat starch

The analysis of the dynamic rheological of buckwheat starch, Fig. 6a and b, illustrated storage modulus (G′), loss modulus (G″), and tan δ (G'' / G′). Influenced by external forces, food will produce deformation, with elastic properties, after the force disappears, with viscosity properties, showing a flow state (Zhang et al., 2022). Fig. 6 a, the modulus values of all buckwheat starches presented in the following order: G' > G″, that showed the samples exhibited solid-like behavior. The SY 12 h group exhibited the highest G′ and G″ with tanδ was lowest. Both modulus values (G′ and G″) of SYLP 6 h were significantly lower ($p < 0.05$) compared to the SY 6 h. The tanδ values for SYLP 6 h and SYLP 12 h were higher than those for SY and NY, which indicated that SYLP fermentation had a bigger influence on viscous than elastic properties (Fig. 6b).

The continuous shear flow curves of the different fermentation treatment groups buckwheat were presented in Fig. 6c. The values for the plotted curves were obtained from the fitted Ostwald–de Waele rheological model and the results were shown in Table S2. The flow index of n < 1 indicated that the shear stress decomposed the gel structure, indicating its shear-thinning behavior. Therefore, it was found that the gel obtained has typical pseudoplastic fluid properties (Pycia et al., 2012). The consistency index K of buckwheat was increased first and then decreased changed with the fermentation time. At 12 h, The K values of SYLP and SY groups were the highest, which were 131.0 and 153.2. The higher K values indicated higher structural strength, resulting in less thixotropic behavior. Both the molecular weight and chemical branch structure of starch were increased, which can be explained by the rise in the hysteresis loop area values. The lengthened synergistic fermentation period may also have increased the number of molecules of starch in a given volume, increasing density. This, in turn, strengthened the entanglement between molecular chains and heightened friction between starch particles. When the internal structure is damaged, starch paste flow resistance rises and its recovery rate declines under the same shear force (Chen et al., 2018; Wang et al., 2022). The hysteresis loop area values were measured for the required energy to resolve the paste or gel structure. Hysteresis loop area values of different treatment groups had no obvious difference. However, in the SYLP group, it increased significantly from 23.6 to 31.8 from 6 h to 12 h < 0.05). It decreased at 24 h, but the difference was not significant. The results indicated that SYLP 12 h starch had the strongest strength in structure, viscosity, thixotropy, gel formation, and recovery ability. The consistency index K and RVA results validated it further.

The thixotropy of starch was critical for the shape retention of starchy foods; however, during the transportation and processing of starch products, the apparent viscosity of starch paste may be affected by intermittent shear force, which increased the mobility of objects and complicates transportation and processing. Therefore, it was critical to research starch thixotropy. In Fig. 6c, at 6 h, the shear stress of the SY and SYLP group was significantly lower than that of natural fermentation and native buckwheat starch. It may be related to the decrease of amylose due to hydrolysis during fermentation. This assumption is also confirmed by Sikora (Sikora et al., 2015). During the 12 h and 24 h fermentation, the SYLP group showed increased shear stress and a significantly higher viscosity than the other groups; the variation tendency of shear stress was in line with K and the dynamic rheological results. The results showed that both the rising and falling curves exhibited shear-thinning behavior. Generally, shear thinning tendency is an important and desirable rheological property in food processing, which facilitates the prevention of settling of the material and contributes to the production of a homogenous system.

4. Conclusions

The resultd showed that SYLP fermentation led to the advancement of the acid production time, which decreased the content of amylose starch in the amorphous zone of buckwheat starch in a short period, and the SEM results indicated that the surface of starch was eroded, and the starch exhibited an increase in the intensity of absorption associated with the - CH_2 -as detected by FT-IR (861-764 cm^{-1}). Therefore , the study showed that SYLP fermentation can shorten the time it takes for the multiscale structure of buckwheat starch to change. The RVA and DSC results indicated that SYLP fermentation reduced the setback, breakdown, and pasting temperature, Tc, and ΔH values. In conclusion, SYLP fermentation is more effective than natural and yeast fermentation. The SYLP fermentation improved the properties of buckwheat starch, especially pasting, which not only facilitates the fermentation of buckwheat-related food products, but also serves as an improved method for better utilization of buckwheat flour. The proposed method can be applied to the production of different products.

CRediT authorship contribution statement

Xia Li: Conceptualization, Investigation, Visualization, Writing – original draft, Methodology. **Shanshan Wei:** Formal analysis, Conceptualization, Investigation, Writing – original draft. **Zixin Gao:** Writing – review & editing. **Ruixue Zhao:** Formal analysis, Writing – review & editing. **Zhanpeng Wang:** Writing – review & editing, Revision. **Yuling Fan:** Supervision, Writing – review & editing. **Linlin Cui:** Writing – review & editing, Supervision. **Yuhua Wang:** Conceptualization, Data curation, Visualization, Supervision.

Declaration of competing interest

The authors declare that they have no known competing financial interests or personal relationships that could have appeared to influence the work reported in this paper.

Data availability

Data will be made available on request.

Acknowledgements

This work was financially supported by Jilin Province Science and Technology Development Plan Project (20220508115RC).

Appendix A. Supplementary data

Supplementary data to this article can be found online at https://doi.org/10.1016/j.crfs.2023.100670.

References

Bian, X., Chen, J., Yang, Y., Yu, D., Ma, Z., Ren, L., Wu, N., Chen, F., Liu, X., Wang, B., Zhang, N., 2022. Effects of fermentation on the structure and physical properties of glutinous proso millet starch. Food Hydrocolloids 123, 107144. https://doi.org/10.1016/j.foodhyd.2021.107144.

Biduski, B., Silva, W.M.F.D., Colussi, R., Halal, S.L.D.M.E., Lim, L.-T., Dias, Á.R.G., Zavareze, E.D.R., 2018. Starch hydrogels: the influence of the amylose content and gelatinization method. Int. J. Biol. Macromol. 113, 443–449. https://doi.org/10.1016/j.ijbiomac.2018.02.144.

Chen, B., Guo, Z., Zeng, S., Tian, Y., Miao, S., Zheng, B., 2018. Paste structure and rheological properties of lotus seed starch–glycerin monostearate complexes formed by high-pressure homogenization. Food Res. Int. 103, 380–389. https://doi.org/10.1016/j.foodres.2017.10.069.

Cheng, W., Gao, L., Wu, D., Gao, C., Meng, L., Feng, X., Tang, X., 2020. Effect of improved extrusion cooking technology on structure, physiochemical and nutritional characteristics of physically modified buckwheat flour: its potential use as food ingredients. LWT 133, 109872. https://doi.org/10.1016/j.lwt.2020.109872.

Dar, M.Z., Deepika, K., Jan, K., Swer, T.L., Kumar, P., Verma, R., Verma, K., Prakash, K. S., Jan, S., Bashir, K., 2018. Modification of structure and physicochemical properties of buckwheat and oat starch by γ-irradiation. Int. J. Biol. Macromol. 108, 1348–1356. https://doi.org/10.1016/j.ijbiomac.2017.11.067.

Gui, Y., Zou, F., Zhu, Y., Li, J., Wang, N., Guo, L., Cui, B., 2022. The structural, thermal, pasting and gel properties of the mixtures of enzyme-treated potato protein and potato starch. LWT 154, 112882. https://doi.org/10.1016/j.lwt.2021.112882.

Han, Y., Du, J., 2023. A comparative study of the effect of bacteria and yeasts communities on inoculated and spontaneously fermented apple cider. Food Microbiol. 111, 104195 https://doi.org/10.1016/j.fm.2022.104195.

Kong, X.-R., Zhu, Z.-Y., Zhang, X.-J., Zhu, Y.-M., 2020. Effects of Cordyceps polysaccharides on pasting properties and in vitro starch digestibility of wheat starch. Food Hydrocolloids 102, 105604. https://doi.org/10.1016/j.foodhyd.2019.105604.

Kumar, G., VanGessel, F.G., Munday, L.B., Chung, P.W., 2023. Correction to "3-phonon scattering pathways for vibrational energy transfer in crystalline RDX.". J. Phys. Chem. 127 (21), 4764–4770. https://doi.org/10.1021/acs.jpca.3c02499.

Ma, S., Wang, Z., Tian, X., Sun, B., Huang, J., Yan, J., Bao, Q., Wang, X., 2022. Effect of synergistic fermentation of Lactobacillus plantarum and Saccharomyces cerevisiae on thermal properties of wheat bran dietary fiber-wheat starch system. Food Chem. 373, 131417 https://doi.org/10.1016/j.foodchem.2021.131417.

Ma, Y., Zhang, W., Pan, Y., Ali, B., Xu, D., Xu, X., 2021. Physicochemical, crystalline characterization and digestibility of wheat starch under superheated steam treatment. Food Hydrocolloids 118, 106720. https://doi.org/10.1016/j.foodhyd.2021.106720.

Molavi, H., Razavi, S.M.A., Farhoosh, R., 2018. Impact of hydrothermal modifications on the physicochemical, morphology, crystallinity, pasting and thermal properties of acorn starch. Food Chem. 245, 385–393. https://doi.org/10.1016/j.foodchem.2017.10.117.

Pycia, K., Juszczak, L., Gałkowska, D., Witczak, M., 2012. Physicochemical properties of starches obtained from Polish potato cultivars. Starch - Stärke 64 (2), 105–114. https://doi.org/10.1002/star.201100072.

Singh, S., Kaur, M., 2017. Steady and dynamic shear rheology of starches from different oat cultivars in relation to their physicochemical and structural properties. Int. J. Food Prop. 20 (12), 3282–3294. https://doi.org/10.1080/10942912.2017.1286504.

Sun, L., Sun, X., Du, Y., Fang, Y., Yang, W., Hu, Q., Pei, F., 2022. Effect of the starch structure fermented by *Lactobacillus plantarum LB-1* and yeast on rheological and thermomechanical characteristics of dough. Food Chem. 369, 130877, 10/gpqg3w.

Wang, J., Zhao, S., Min, G., Qiao, D., Zhang, B., Niu, M., Jia, C., Xu, Y., Lin, Q., 2021. Starch-protein interplay varies the multi-scale structures of starch undergoing thermal processing. Int. J. Biol. Macromol. 175, 179–187. https://doi.org/10.1016/j.ijbiomac.2021.02.020.

Wang, N., Huang, S., Zhang, Y., Zhang, F., Zheng, J., 2020. Effect of supplementation by bamboo shoot insoluble dietary fiber on physicochemical and structural properties of rice starch. LWT 129, 109509. https://doi.org/10.1016/j.lwt.2020.109509.

Wang, Q., Li, L., Zheng, X., 2020. A review of milling damaged starch: generation, measurement, functionality and its effect on starch-based food systems. Food Chem. 315, 126267 https://doi.org/10.1016/j.foodchem.2020.126267.

Wang, Y., Bai, Y., Ji, H., Dong, J., Li, X., Liu, J., Jin, Z., 2022. Insights into rice starch degradation by maltogenic α–amylase: effect of starch structure on its rheological properties. Food Hydrocolloids 124, 107289. https://doi.org/10.1016/j.foodhyd.2021.107289.

Zabot, G.L., Silva, E.K., Emerick, L.B., Felisberto, M.H.F., Clerici, M.T.P.S., Meireles, M.A. A., 2019. Physicochemical, morphological, thermal and pasting properties of a novel native starch obtained from annatto seeds. Food Hydrocolloids 89, 321–329. https://doi.org/10.1016/j.foodhyd.2018.10.041.

Zhang, J., Zhang, M., Wang, C., Zhang, Y., A, R., Bai, X., Zhang, Y., Zhang, J., 2022. Effects of high hydrostatic pressure on microstructure, physicochemical properties and in vitro digestibility of oat starch/β-glucan mixtures. International Journal of Food Science & Technology 57 (4), 1888–1901. https://doi.org/10.1111/ijfs.15055.

Zhang, Y., Li, G., Wu, Y., Yang, Z., Ouyang, J., 2019. Influence of amylose on the pasting and gel texture properties of chestnut starch during thermal processing. Food Chem. 294, 378–383. https://doi.org/10.1016/j.foodchem.2019.05.070.

Zhou, X., Xing, Y., Meng, T., Li, J., Chang, Q., Zhao, J., Jin, Z., 2021. Preparation of V-type cold water-swelling starch by ethanolic extrusion. Carbohydrate Polymers 271, 118400. https://doi.org/10.1016/j.carbpol.2021.118400.